# A Test Facility for Hypervelocity Rarefied Flows

## M. N. Macrossan, H-H. Chiu and D. J. Mee

*Centre for Hypersonics, The University of Queensland, Brisbane 4072 Australia.*

**Abstract.** This paper describes a rarefied hypervelocity test facility producing gas speeds greater than 7 km/s. The X1 expansion tube at The University of Queensland has been used to produce nitrogen flows at 8.9 and 9.5 km/s with test flow durations of 50 and 40 μs respectively. Rarefied flow is indicated by values of the freestream breakdown parameter > 0.1 (Cheng's rarefaction parameter < 10) and freestream Knudsen numbers up to 0.038, based on a model size of 9 mm. To achieve this, the test gas is expanded from the end of the acceleration tube into a dump tank. Nominal conditions in the expansion are derived from CFD predictions. Measured bar gauge (Pitot) pressures show that the flow is radially uniform when the Pitot pressure has decreased by a factor ten. The measured bar gauge pressures are an increasing fraction of the expected Pitot pressure as the rarefaction parameters increase.

## 1 INTRODUCTION

Compared to other areas of fluid mechanics, there is a paucity of experimental data for the aerodynamics of rarefied gases. The Direct Simulation Monte-Carlo (DSMC) method (Bird 1994) has assumed the role of surrogate for experiments (Muntz 1989). It is very important that the accuracy of DSMC be assessed in the extreme conditions presented by aerobraking manoeuvres where the collision models will be severely tested. Present experimental facilities for rarefied gas flows are limited to stagnation temperatures of about 2000 K and hence are limited to test speeds of about 2 km/s. The development of a high-speed test-facility that spans the range from rarefied to continuum flow will represent a significant increase in the range of experimental testing for DSMC. This paper describes how the X1 expansion tube of the Centre for Hypersonics at the University of Queensland has been used to produce such flows.

## 2 CONDITIONS FOR RAREFIED HYPERVELOCITY FLOWS

In the case of the flow around an object such as an aerobraking shield, the importance of rarefaction is indicated by the ratio of the collision time, $\tau$, to the characteristic flow time $D/u$, where $D$ is the characteristic size of the object and $u$ is the characteristic flow speed relative to the object. This ratio can be expressed as $\pi^{1/2}S\lambda/(2D) = (\pi^{1/2}/2)KnS$ where $\lambda$ is the mean free path and $S$ is the speed ratio. Since the nominal mean free path can be related to viscosity by $\lambda = 2\mu/(\rho\sqrt{8RT/\pi})$, we can express the Knudsen number as $Kn = \pi^{1/2}S/\mathrm{Re}$, and the "rarefaction ratio" above as $(\pi/2)S^2/\mathrm{Re}$. This ratio can also be expressed as $\approx \mu u/(\rho RTD)$ and, since the typical shear stresses in the flow is $\approx \mu U/D$, it is proportional to the ratio of the shear stress to the pressure. This ratio is the same as Bird's breakdown parameter for steady flow, $P$, (Bird 1994) but with the length-scale equal to the characteristic model size. It is convenient to drop the constant $\pi/2$, and to define a "rarefaction" or breakdown parameter as $P_D \equiv S^2/\mathrm{Re}$. This parameter, in the form $M^2/\mathrm{Re}$ (Tsien 1946, Clayden 58, Hurlbut 58) and in the form $M^2/\sqrt{\mathrm{Re}}$, which may be interpreted as a Knudsen number based on the characteristic boundary layer thickness (Schaaf and Chambre 49), has been used to provide a criteria for the breakdown of the continuum equations.

Since the merged shock-boundary layer would be expected to dominate a rarefied flow about any test model in the flow, the breakdown parameter evaluated for conditions behind the bow shock, rather than for freestream conditions, might be the better indicator of rarefied conditions. A parameter derived directly from the theory of the merged shock-boundary layer is Cheng's (1961) rarefaction parameter, $\chi = p_\infty D/(\mu_\infty U_\infty C^*)$, where $C^* = \mu^* T_\infty/(\mu_\infty T^*)$, $T^* = (T_s + T_w)/2$, $T_s$ is the post-shock temperature, $T_w$ is the wall temperature and $T^*$ is a characteristic temperature in the merged layer between the bow shock and blunt body. Note that $\chi \approx (Kn_\infty S_\infty C^*)^{-1}$, and is thus related to the freestream breakdown parameter modified slightly to account for typical conditions in the merged shock-boundary layer. The parameter $\chi$ has been used to correlate experimental aerodynamic coefficients on blunt bodies in rarefied flow (for example Coleman, Metcalf and Berry, 1977). The results show that rarefied effects can be expected to become important for $\chi < 10$. Accordingly, the aim of this work is to produce a test flow speed in excess of earth orbital speed (7 km/s) with $\chi < 10$. This implies values of the freestream breakdown parameter $P_D \approx \chi^{-1} > 0.1$ and corresponds to fewer than 10 collisions/molecule as the flow traverses the characteristic length. To calculate the nominal mean free path and Reynolds number, we have used the expressions for the high temperature viscosity of a mixture of molecular and atomic nitrogen given by Gupta *et al* (1989).

# 3 EXPERIMENTAL DETAILS AND CALIBRATION

The experiments were performed in the X1 free-piston driven expansion tube (see Fig. 1) with nitrogen as the test gas. X1 is capable of producing flows at speeds up to 15 km/s. The acceleration tube diameter is 38 mm and the test time is limited to the order of tens or hundreds of microseconds. To produce rarefied hypervelocity flow, low initial filling pressures are used for the test gas and acceleration gas, and the flow produced at the exit of the tube is expanded further as a free jet expanding into the low pressure background gas in the dump tank. The test gas was pure nitrogen.
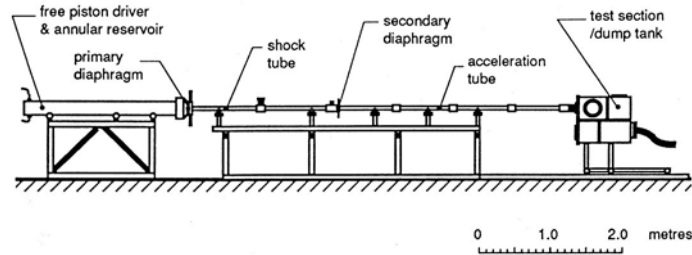


**FIGURE 1** Schematic of the X1 Superorbital expansion tube

The flow conditions at the exit plane of the expansion tube were calculated using the TUBE program (Neely 1996, Neely and Morgan 1994). Conditions are calculated from the tube filling pressures and measurements of the shock speeds in the shock and acceleration tubes. One-dimensional flow in chemical equilibrium is assumed. Further details can be found in the references listed above. The uncertainty in the calculated Pitot pressure is dominated by the uncertainty in the speed of the shock down the acceleration tube. With an estimated uncertainty in shock speed of +/- 1% an uncertainty of +/-10% results in the predicted Pitot pressure. Two flow conditions were considered and the nominal (average) conditions at the exit of the acceleration tube are shown in Table 1. The nitrogen gas is partially dissociated and the chemical recombination length $u/(d\alpha/dt)_{rec}$, where $u$ is the flow speed, was in excess of 1km, so the chemical composition remains frozen in the expansion. The Pitot pressures for all experimental results reported here were within 10% of the nominal values in table 1. The flow conditions after expansion were estimated from CFD calculations, as explained below.

The flowfield of the free jet expansion into the dump tank was surveyed using bar gauges designed specifically for the present application. Surveys were made at distances from 25 to 340 mm from the exit of the acceleration tube. Bar gauges are used to give a fast-response Pitot pressure measurements in impulsively starting flows. They were used in preference to conventional Pitot probe/pressure transducer arrangements because of the poor response of such probes in the low density, short duration flows of the present study.

**Table 1** Nominal flow conditions at exit of X1 expansion tube

| Condition | Density $\rho$ (kg/m$^3$) | Flow speed u (m/s) | Temperature (K) | Mach number M | Mass fraction $\alpha$ | Pitot (kPa) |
|-----------|------------------|------------|--------------|-------------|-------------|---------|
| I | 8.4 x 10$^{-3}$ | 8900 | 5700 | 5.6 | 0.12 | 626.8 |
| II | 2.2 x 10$^{-3}$ | 9500 | 5500 | 6.1 | 0.12 | 186.7 |

The bar gauges for the present study are shown in Fig. 2. They are a modified form of the conventional bar gauge. A steel disc of 9 mm diameter and 1 mm thickness is attached to the front of the bar. This is done to improve the aerodynamic shielding of the bar and to improve the survivability of the gauge. The addition of a disc will slow the response of the bar gauge, however with the present arrangement the rise time of the gauge is still only about 5 μs.
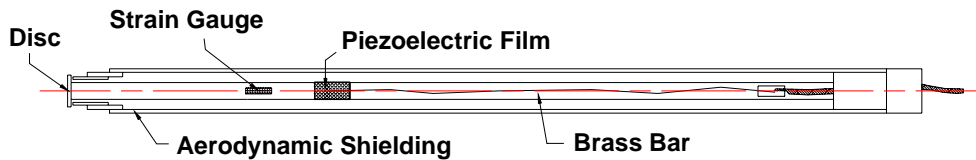


**FIGURE 2** Bar gauge design for the present experiments.

The strain sensing elements used for the present tests were piezoelectric polymer film (Smith and Mee 1996) and semiconductor strain gauges. The piezoelectric film, of 10 mm length in the axial direction, was wrapped around the brass bar with the most sensitive axis of the film being aligned with the axis of the bar. Two strain gauges (Kulite type ACP-120-300) were mounted on opposite sides of the bar in a bending compensation arrangement so that axial strain in the bar was measured. These gauges have an active length of 8 mm. The strain gauge amplifier used had a rise time of 1 μs. It was found that the piezoelectric film gauge deteriorated with repeated use but that the semiconductor strain gauge did not show such a trend.

The bar gauges were calibrated using PCB impact hammers (type 086-C04 and 086-D80) which were used to apply measurable forces to the disc of the bar gauges. The time history of force indicated by the hammer was normalized by the voltage indicated by the strain gauge on the stress bar with an appropriate time delay for the propagation of stress waves from the front disc to the strain measurement location. During the first 100 μs after initial hammer impact a constant ratio was obtained and a calibration factor (voltage per unit force) was determined. The accuracy of the calibration obtained from such tests is estimated to be +/- 5%.

These calibrations were checked by placing the bar gauge in a known flow produced by a shock tube and the measured average pressures behind the shock are compared with the expected Pitot pressure in Fig. 3.
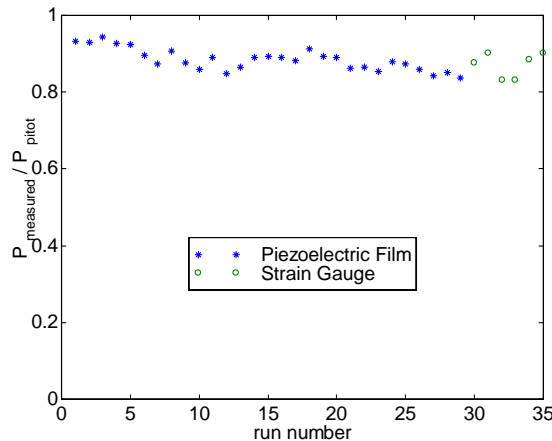


**FIGURE 3** Measured bar gauge pressures after passage of shock, compared with theoretical Pitot pressure

A curved bow shock is formed in front of the probe, the pressure varies over the disk from close to the Pitot pressure near the centre of the disc to lower pressures towards the edges of the disc. Hence there is a difference between the average pressure acting over the surface of the disc and the Pitot pressure of the flow. Continuum and DSMC calculations (Bourque 1999) show that the ratio of average to Pitot pressure varies from about 0.9 or less for continuum conditions to about 0.95, depending on the Knudsen number. Since the average pressure as a fraction of Pitot pressure generally decreased with run number (successive runs) there is a suggestion of some deterioration in the response of the piezoelectric film gauges with repeated use.

Based on the shock tube tests, it is estimated that the overall uncertainty in the measurement of disc average pressure is +/- 7% for average pressures of the order of 300 kPa, typical of those at exit of the expansion tube. However at greater distances from the tube exit, where the Pitot pressure drops to as low as 3% of that at the exit plane, the uncertainty in the bar gauge measurements will increase. Uncertainty in disc average pressure is estimated to increase to +/- 15% at distances as far as nine tube diameters from the exit plane.



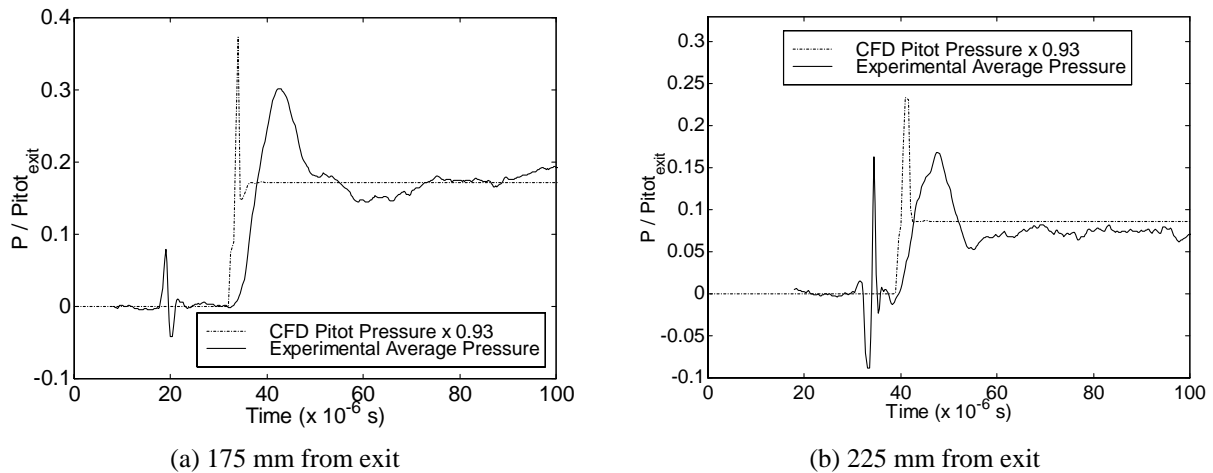(a) 175 mm from exit          (b) 225 mm from exit

**FIGURE 4** Comparison of measured bar gauge pressure time history with CFD predictions (14mm off axis). Traces are average disc pressure normalized with the value predicted at the tube exit. Both traces are from the semiconductor strain gauges.

Example time histories obtained from the bar gauges in the dump tank are given in Fig. 4. A large spike in the signal from the strain sensing devices on the bar gauges was recorded when the flow arrived at the location of the bar gauges (note the spikes at 20 μs in 4a and at 35 μs in 4b). The spike was typically about 10μs duration. This noise was detected with both the piezoelectric film and the semiconductor strain gauges. Experiments confirmed that this was not a pressure signal and the noise is attributed to ionization in the flow when it stagnates at the disc of the bar gauges. The noise level could be reduced with high excitation voltages for the semiconductor gauges but could not be eliminated. The effects of this spike could be moved so they did not interfere with the strain signal by placing the gauge further from the front of the bar gauge. Because of the finite time taken for the stress waves to travel from the front of the bar to the gauge location, moving the gauge further down the bar allows the spike to be separated from the pressure signal, as can be seen in Fig. 4.


# 4 CFD METHOD AND RESULTS


CFD calculations of the expansion of the flow from the exit of the expansion tube into the dump were made with a multi-block Navier-Stokes/Euler code (Jacobs 89), in "Euler" or inviscid mode. The mixture gas constant was R = 332 J kg$^{-1}$ K$^{-1}$ (12% dissociation) and γ = 1.333. These calculations were intended to give an indication of whether quasi-steady, rarefied flow conditions could be expected in the dump tank. Figure 5 shows the unsteady expansion of the jet in the dump tank. The grid is axis-symmetric and the figure shows the end of the acceleration tube protruding into the dump tank. Uniform and steady inflow conditions (as shown in Table 1) were set in the acceleration tube. Where this high speed flow meets the low pressure rest gas in the dump tank, it is partially reflected to form an upstream facing shock which is swept downstream, and a shock is propagated through the low pressure gas. The

results indicate that the jet is reflected from the sides of the dump tank, but the reflected shock so formed does not interfere with the core flow within the test time available.
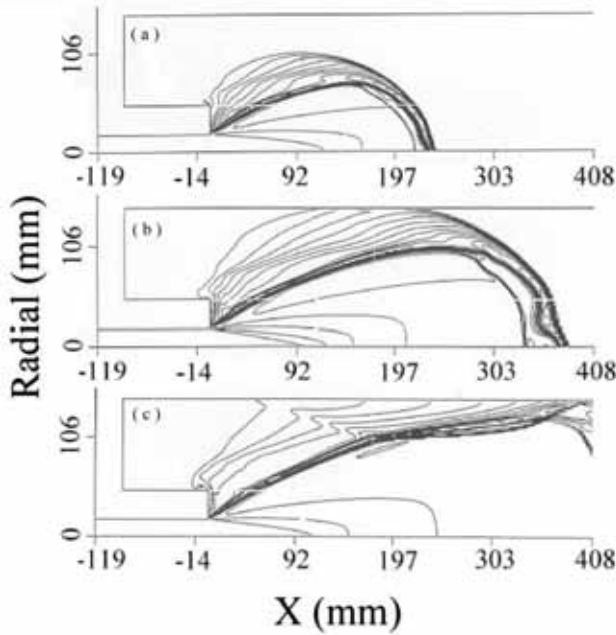


**FIGURE 5** Computed pressure contours at time (a) 40 μs, (b) 60 μs and (c) 80 μs after flow start.



**FIGURE 6** Rarefaction parameters, flow about bar gauge (9 mm ϕ), condition I, CFD predictions: $\chi_D^{-1}$, $P_D$, $Kn_D$ v axial distance from tunnel exit. Also reaction rate parameter behind a normal shock.

Sample time histories of $0.93 \times$ Pitot pressure obtained from the simulations are compared with the measured time histories from the bar gauges in Fig. 4. The factor 0.93 is a nominal value applied to all the CFD results reported here, to account for the difference between Pitot pressure and the average pressure on the face of the disc of the bar gauges (see section 3.1). The traces have been lined up so that the pressure rises at the same time for both the computed and measured signals. Note also that experimental pressures are normalized by the value measured at the exit plane of the tube, while the CFD Pitot pressure traces are normalized by the Pitot pressure for the nominal conditions at the exit plane used in the simulation. Both traces show an initial overshoot in pressure as the starting shock propagates down the dump tank. The level of the overshoot is higher and the duration shorter for the computed traces. At least part of this difference, but not all, can be attributed to the limited response time of the bar gauges. This trend was consistent throughout the measurements. The final levels are similar.

Fig. 6 shows the rarefaction parameters evaluated for the freestream conditions predicted by CFD along the centerline of the expansion, at different axial distances from the exit of the expansion tube, for the higher density flow condition I. The inverse of Cheng's rarefaction parameter is shown to show its close relationship to the breakdown parameter. Rarefaction effects can be expected at an axial distance of 220mm into the expansion, where $\chi_D < 10$, $P_D > 0.1$ and $Kn_D > 0.01$. The figure also shows the reaction rate parameter, $L_{chem}/D$, where $L_{chem} = u/(d\alpha/dt_s)^{-1}$ and the dissociation rate is evaluated for conditions behind a normal shock. The low values of this parameter imply that the flow around the bar gauge should be in chemical equilibrium, expect perhaps far into the expansion, for values $> 0.1$, where some chemical non-equilibrium effects might be expected. This assumption of chemical equilibrium must be tentative only since, if the reaction rate parameters measured by Kewley and Hornung (1974) are used, rather than those of Gupta et al (1989), the reaction rate parameter is larger, 0.7 at x = 225mm, which implies a highly non-equilibrium chemical flow.
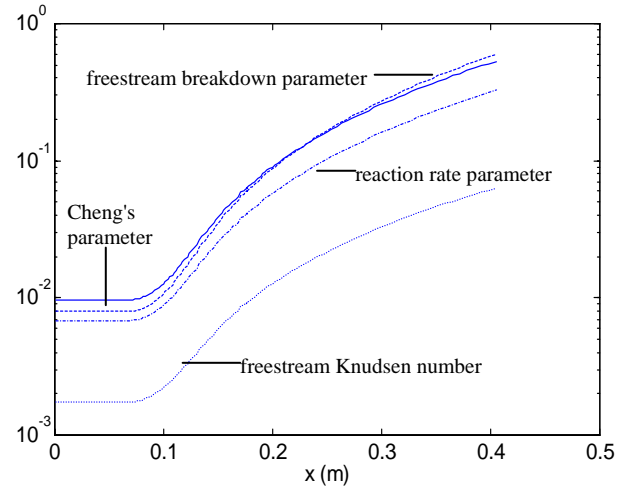
## 5 EXPERIMETAL RESULTS

The result of the survey results for condition I is shown in Figure 7. The average pressure on the disc of the bar gauge at the traverse location is normalized with the Pitot pressure predicted at the exit of the acceleration tube, which varied from the nominal conditions from shot to shot. It can be seen that a core of high Pitot pressure remains

near the centre-line until 175 to 225 mm from the exit plane. At 225 mm, where rarefaction is expected, the Pitot pressure is uniform to within experimental uncertainty. The results show that while there are strong axial gradients in the Pitot pressure, the radial variation is small at this distance into the dump tank. At some locations, repeat shots were made. The results in Fig. 7 are averages of all data obtained at each location.
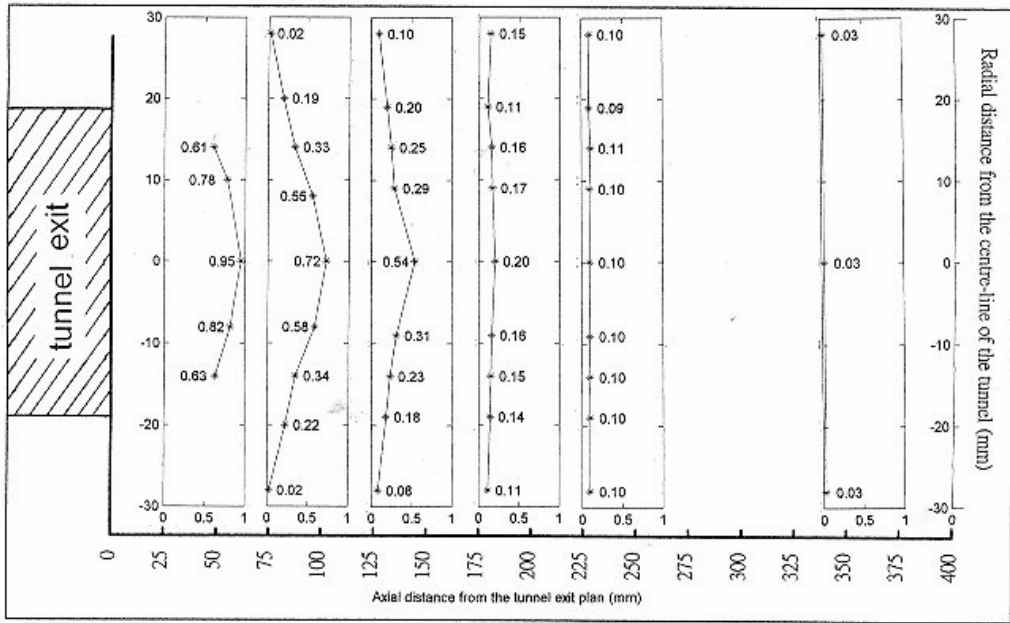


**FIGURE 7**. Measured bar-gauge pressures in free jet expansion, normalized by the Pitot pressure at the tunnel exit.



(a) x = 125 mm, $Kn_D = 0.003$, $\chi_D = 45$    b) x = 225 mm., $Kn_D = 0.017$, $\chi_D = 8$
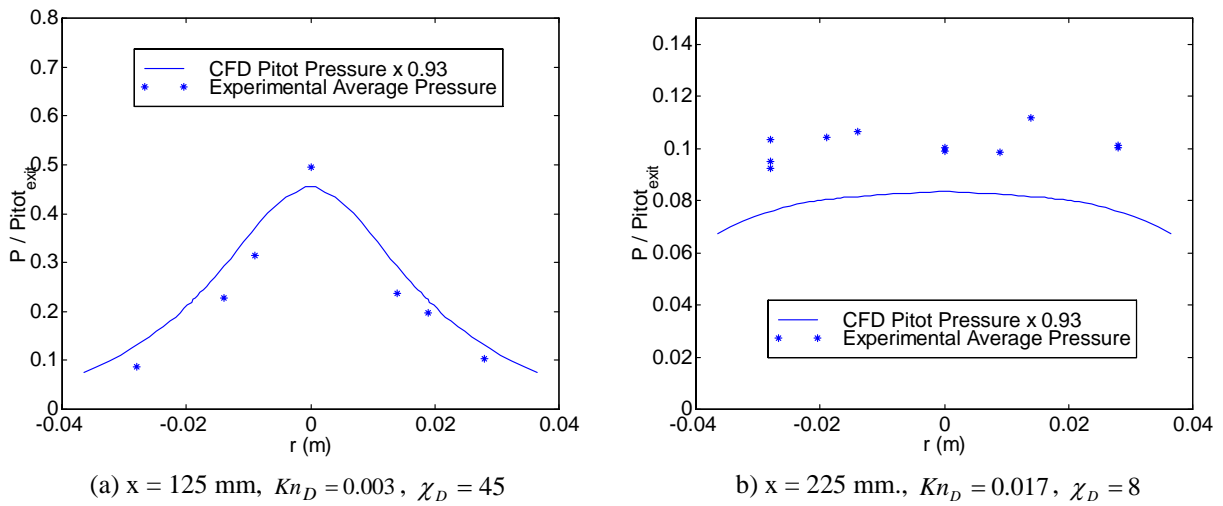
**FIGURE 8** Bar-gauge pressures & CFD predictions in expansion, normalized by the Pitot pressure at the tunnel exit. Cond. I.

Examples of traverses showing results from all shots are shown for traverse planes at 125 mm and 225 mm in Fig. 8. These are compared with results derived from the continuum CFD calculations of the jet expansion into the dump tank that provided nominal conditions in the expansion. The Pitot pressures obtained from the simulation have been multiplied by a nominal factor of 0.93 to compare with the bar gauge pressures. For the plane at 225 mm, the measured bar gauge pressure Pitot profile in Fig. 8(b) indicates there is a central core flow of radius 25 mm

where conditions are approximately constant. The CFD results show that the flow divergence angle increases linearly from zero at the axis to $4^{o}$, and the flow density decreases to 95% of the central value, at r = 25 mm, while the flow speed and temperature change by only 1% in this core region. The uniformity in the temperature is easily seen from the contours in Fig. 5. The measured bar gauge pressures show a scatter of approximately +/- 15% in line with the uncertainties in the measurements of bar gauge and Pitot pressures. Nevertheless, the measured pressures are noticeably greater than the expected average pressure (0.93 x Pitot pressure) at this location, whereas they were generally less at the plane at 125 mm shown in Fig 8(a). This is consistent with onset of rarefaction effects between these two locations, where the drag coefficient begins to increases towards free-molecular values. The nominal flow conditions at x = 225 mm are $\rho = 6.9 \times 10^{-4} kg/m^3$, $u = 9370 m/s$, $T = 2470K$, $Kn_D = 0.017$, $P_D = 0.13$ and $\chi_D = 8$, with D equal to the bar gauge diameter of 9mm.

For the low pressure case II, the conditions at this location are shown in Fig. 9. The nominal freestream flow conditions in this case are $\rho = 2.2 \times 10^{-4} kg/m^3$, $u = 9900 m/s$, $T = 2560K$, $Kn_D = 0.053$, $P_D = 0.41$ and $\chi_D = 2.48$. These conditions are more rarefied and the measured bar gauge pressures are a much larger fraction of expected Pitot pressure, again consistent with the assumption of rarefied flow around the bar gauge.
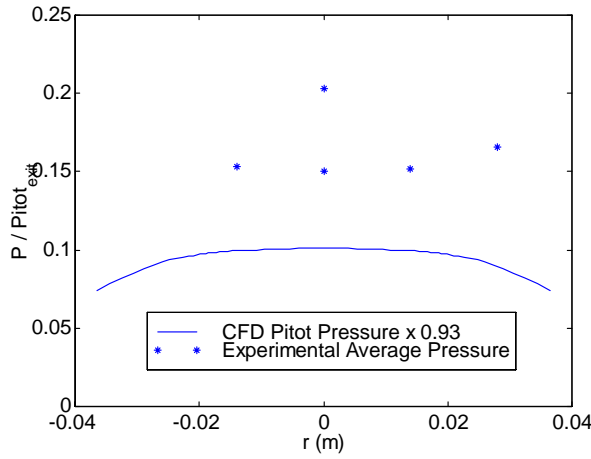


**FIGURE 9** Measured bar-gauge pressures and CFD predictions in free jet expansion, normalized by the Pitot pressure at the tunnel exit in each case. Condition II, x= 225 $Kn_D = 0.053$, $\chi_D = 2.48$
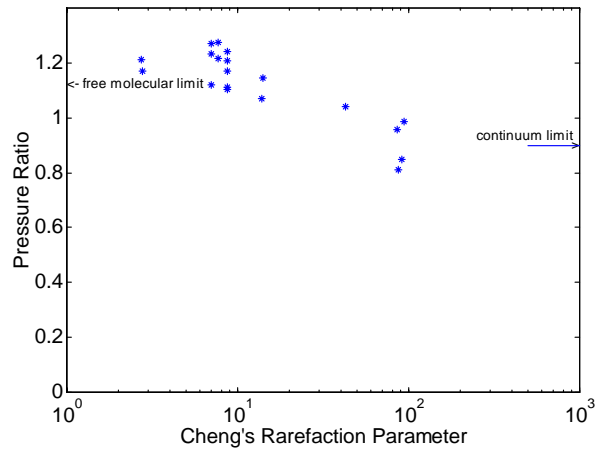
**FIGURE 10** Measured bar gauge pressure $v$ Cheng's rarefaction parameter, normalized w.r.t. CFD Pitot pressure. Conditions I & II

All the measured pressures, normalized with respect to the CFD predicted pitot pressure

$$\left(P_{x,bar} / Pitot_{exit}\right)_{meas} / \left(Pitot_x / Pitot_{exit}\right)_{CFD}$$

are shown in Fig. 10, as a function of Cheng's rarefaction parameter, also derived from CFD. Since only two CFD calculations were made, one for each nominal condition, the rarefaction parameters for the experimental measurements have been estimated from the nominal value by correcting for the deviation in density, flow speed and temperature from the nominal value in each case. The data shows the expected increase in measured pressure as the rarefaction increases. The measured values greater than the expected free molecular values probably indicate that the flow conditions (and hence free molecular limiting values) are not known sufficiently accurately from the CFD calculations. The anomalous (low) results at $\chi = 100$ were obtained after the bar-gauges had been used many times and it is possible the piezoelectric film may have deteriorated.


# 6 CONCLUSIONS

The experiments and CFD simulations presented here have shown that a rarefied hypervelocity flow can be produced using the X1 expansion tube, by operating at lower than normal pressures and by expanding the flow produced by X1 in the dump tank. A quasi-steady core region of approximately 50 mm diameter is produced, with a

divergence in the velocity vector of less than $4^o$, and variation in density of 5% across the core region. The flow time is long enough to measure the forces acting on a test model with a nominal size of 9mm (in this case a bar gauge). Values of the freestream breakdown parameter of > 0.1 and Cheng's rarefaction parameter of 10 or less indicate that rarefied flow conditions can be expected. The measured values of bar gauge pressure for values of Cheng's parameter greater than 10 are consistent with the onset of rarefied flow

For future work, further surveys using semiconductor strain gauges as the sensing elements for the bar gauges are planned. Also, more accurate CFD simulations are being undertaken to determine the flow conditions in the expansion. Improvements will be made in two areas. First the shock tube exit conditions can be determined from an accurate CFD simulation of the operation of the expansion tube, including the effects of viscosity and finite rate chemistry. This preliminary calculation will provide the upstream flow conditions (at the entrance to the dump tank), including the boundary layers formed in the expansion tube, for any CFD calculation of the expansion in the dump tank. The second improvement will be in the calculation of the flow in the dump tank; both Navier-Stokes calculations and direct simulations (particle based) calculations of the expanding flow will be undertaken, the later using DSMC or the specialized particle methods for high density flows (Macrossan 2000 a & b).

# REFERENCES

1. BIRD, G A. "Rarefied gas dynamics and the direct simulation of gas flows" Clarendon Press, Oxford, 1994.
2. BORQUE, B. "Development of a hypervelocity wind tunnel for rarefied flows", Undergraduate thesis, Department of Mechanical Engineering, The University of Queensland, 1999.
3. CHENG, H K. "Hypersonic shock-layer theory of the stagnation region at low Reynolds Number" *Proc 1961 Heat Transfer and Fluid Mechanics Institute* (Stanford University Press, Stanford, California), 1961.
4. CLAYDEN, W A. "The ARDE low-density wind tunnel" *1st Int Symposium Rarefied Gas Dynamics* (ed Devine), 21, Pergamon Press 1958.
5. COLEMAN, G T, METCALF, S C and BERRY, C J. "Heat transfer to hemisphere cylinders and bluff cylinders between continuum and free molecular limits" *10th Int Symposium Rarefied Gas Dynamics* (ed Potter), Part I, 393, 1977.
6. GUPTA, R YOS, J M, THOMPSON, R A and LEE, K-P. "A review of reaction rates and thermodynamic and transport properties for the 11-species air model for chemical and thermal non-equilibrium calculations to 30000K" *NASA TM-101528*, 1989.
7. HURLBUT, F C. "Techniques of measurement, flow visualisation". *1st Int Symposium Rarefied Gas Dynamics* (ed Devine), 55, Pergamon Press 1958.
8. JACOBS, P A. "MB_CNS: A computer program for the simulation of transient Compressible Flows," Department of Mechanical Engineering Report 1/89, University of Queensland, 1989.
9. KEWLEY, D J and HORNUNG, H G. "Free-piston shock-tube study of nitrogen dissociation". *Chem Phys Lett* 25, 531, 1974.
10. MACROSSAN, M. N. "A particle simulation method for the BGK equation", presented *at 22nd Int Symposium on Rarefied Gas Dynamics*, Sydney July 2000a.
11. MACROSSAN, M. N. "A particle-only hybrid method for near continuum flows", presented at *22nd Int Symposium on Rarefied Gas Dynamics*, Sydney July 2000b.
12. MUNTZ, E P. "Rarefied gas dynamics", *Ann Rev Fluid Mech*, **21**, 387, 1989.
13. NEELY, A. "Experimental and analytical study of a pilot superorbital expansion tube for aerothermodynamic testing to 13 km/s in air". Ph D Thesis, The University of Queensland, 1996.
14. NEELY, A, MORGAN, R. "The superorbital expansion tube concept, experiment and analysis". *Aero J*, **March** 1994, 97, 1994.
15. SCHAAF, S A and CHAMBRE, P L. "Flow of rarefied gases". *High speed Aerodynamics and Jet Propulsion Series*, III (H). Princeton University Press, 1949.
16. SMITH, A L, MEE, D J . "Dynamic strain measurement using piezoelectric polymer film". *J Strain Anal*, **31**(6), 463, 1996.
17. TSEIN, H S. "Superaerodynamics, mechanics of rarefied gases". *J Aero Sci*, **13**, 342, 1946.